



Editor's choice
Scan to access more
free content

EXTENDED REPORT

Proof of concept: enthesitis and new bone formation in spondyloarthritis are driven by mechanical strain and stromal cells

Peggy Jacques,¹ Stijn Lambrecht,¹ Eveline Verheugen,¹ Elin Pauwels,² George Kollias,³ Maria Armaka,³ Marleen Verhoye,⁴ Annemie Van der Linden,⁴ Rik Achten,⁵ Rik J Lories,⁶ Dirk Elewaut¹

Handling editor Tore K Kvien

► Additional material is published online only. To view please visit the journal online (<http://dx.doi.org/10.1136/annrheumdis-2013-203643>).

For numbered affiliations see end of article.

Correspondence to

Dr Peggy Jacques or Dr Dirk Elewaut, Laboratory for Molecular Immunology and Inflammation, Ghent University Hospital, Department of Rheumatology, De Pintelaan 185, Ghent 9000, Belgium; Peggy.jacques@ugent.be or dirk.elewaut@ugent.be

Received 18 March 2013
Revised 20 June 2013
Accepted 14 July 2013
Published Online First
6 August 2013

ABSTRACT

Objectives Spondyloarthritis (SpA) are characterised by both peripheral and axial arthritis. The hallmarks of peripheral SpA are the development of enthesitis, most typically of the Achilles tendon and plantar fascia, and new bone formation. This study was undertaken to unravel the mechanisms leading towards enthesitis and new bone formation in preclinical models of SpA.

Results First, we demonstrated that TNF^{AARE} mice show typical inflammatory features highly reminiscent of SpA. The first signs of inflammation were found at the entheses. Importantly, enthesitis occurred equally in the presence or absence of mature T and B cells, underscoring the importance of stromal cells. Hind limb unloading in TNF^{AARE} mice significantly suppressed inflammation of the Achilles tendon compared with weight bearing controls. Erk1/2 signalling plays a crucial role in mechanotransduction-associated inflammation. Furthermore, new bone formation is strongly promoted at enthesal sites by biomechanical stress and correlates with the degree of inflammation.

Conclusions These findings provide a formal proof of the concept that mechanical strain drives both enthesal inflammation and new bone formation in SpA.

INTRODUCTION

Spondyloarthritis (SpA) are a group of chronic inflammatory disorders characterised by asymmetrical peripheral arthritis predominantly of lower limbs, and axial inflammation (sacroiliitis and spondylitis). The disease is typically accompanied by a variety of extra-articular manifestations, such as intestinal and ocular inflammation. In European countries, the overall incidence is estimated at 0.5%–2% of the Caucasian population, with onset frequently in the early adulthood.^{1–2} Inflammation of attachment sites of ligaments and tendons to bones, enthesitis, is a hallmark of SpA which distinguishes it from other inflammatory rheumatic disorders.³ In addition, SpA is also characterised by new bone formation evolving into ankylosis, or into the formation of enthesophytes that also appear to originate from these insertion sites.⁴ Radiographic progression of disease reflecting structural damage is characterised by new bone formation leading to sacroiliac and spinal ankylosis. Both inflammation and progressive structural damage contribute to the burden of disease.⁵

The entheses are subjected to repetitive biomechanical stressing forces that are applied during the course of normal muscle, ligament and tendon action; this suggests a link between biomechanical stress and SpA. McGonagle *et al*⁶ proposed an enthesitis-based model for the pathogenesis of SpA where interactions between biomechanical factors and the innate immune response (eg, to bacterial products) may lead to disease. Nevertheless, the enthesitis concept has remained controversial as synovitis and bone marrow inflammation are also typical signs of active SpA. The anatomical proximity and the ample molecular and cellular communications between these tissues suggest their functional relationship in the pathogenesis of synovitis in SpA with the disease processes defined in the context of the synovio–enthesal complex.⁷

Within this microenvironment, it has become clear that in SpA patients, new bone formation often occurs in close relationship with the entheses. Spinal syndesmophytes develop along the anterior intervertebral ligaments, and bony spurs are formed at the Achilles tendon and plantar fascia.

Interestingly, the process of inflammation and subsequent bone erosion appeared in anatomically distinct sites as compared with new bone formation at the Achilles' enthesis.⁸ Erosions preferentially developed in regions undergoing compression, whereas spur formation occurred in regions prone to tensile forces. These anatomical data further corroborate current paradigms that strongly suggest a molecular uncoupling of inflammation and new bone formation in SpA. Despite a proven efficacy on inflammatory signs and symptoms, treatment with tumour necrosis factor (TNF) blocking agents in mouse models and in patients does not substantially affect progression of ankylosis.^{9–11}

Currently, it remains elusive whether inflammation and new bone formation are closely linked or rather uncoupled, and why these processes colocalise at enthesal sites.

In the current study, we hypothesised that biomechanical factors drive inflammation and new bone formation at enthesal sites. This hypothesis was studied in the TNF^{AARE} mouse model in which chronic and deregulated TNF production leads to arthritis and a Crohn's-like ileitis.^{12–14} We previously argued that this model, depending on endogenous TNF, involving peripheral and axial



► <http://dx.doi.org/10.1136/annrheumdis-2013-203924>

To cite: Jacques P, Lambrecht S, Verheugen E, *et al.* *Ann Rheum Dis* 2014;**73**:437–445.

joints and presenting extra-articular manifestations such as bowel inflammation, is a true translational model of SpA.¹³ Here, we observed that enthesitis is an early feature of this murine model, and that its development is dependent upon biomechanical strain. Bone new formation at enthesal sites, another prominent feature of SpA, was also associated with weight bearing and biomechanical strain. Altogether, these data substantiate the hypothesis that enthesal inflammation and new bone formation are driven by biomechanical strain.

MATERIALS AND METHODS

Animals and housing

TNF^{ARE} mice were provided by Kollias G.¹² CAIA was induced with ArthritoMab from MD Biosciences according to the manufacturer's instructions. All mice were bred and housed in specific pathogen-free conditions in accordance with the general recommendations for animal breeding and housing, and all experiments were conducted in conditions according to the Ethical Committee of Animal Welfare. For treatment with MAPK inhibitors, mice were injected daily with 50 µg/g of PD98059, a selective Erk1/2/MEK1 inhibitor to inhibit Erk1/2 signalling, or SB203580 for p38 blockade (both LC Laboratories) intraperitoneally, or with DMSO as a negative control.

Histology

Murine paws and spine were dissected, fixed in 4% formaldehyde, decalcified in 0.5 M ethylenediamine tetraacetic acid (Sigma-Aldrich, St Louis, Missouri, USA) at 4° or in 5% formic acid until bones were pliable. Paraffin sections were stained with H&E for evaluation of inflammation and bone erosions, or with safranin-O for cartilage appreciation. Enthesitis of Achilles tendon was evaluated by two blinded assessors, and scored on three parameters, infiltrate in the Achilles tendon, calcaneal erosion and exudate at the synovio-enthesal complex, each ranging from 0 (normal) to 3. A composite score was built from these parameters. In addition, digital image analysis was performed by AxioVision software (Carl Zeiss MicroImaging GmbH, Göttingen, Germany). Extent of inflammation within the synovio-enthesal complex was normalised to the size of the growth plate. In a subgroup of mice from tail suspension experiments, inflammation in front paws was also evaluated as follows: absence (0) or presence (1) of dactylitis and enthesitis.

Western blotting

Achilles tendons were dissected on ice, snap frozen and lysed in laemli buffer by a bead-beating procedure to liberate proteins. Immunoblotting using chemiluminescent detection for phospho-Erk1/2 and total Erk1/2 was conducted as previously described. Briefly, equal amounts were loaded on precast 10% SDS-PAGE Criterion gels (Bio-Rad Laboratories, Hercules, California, USA). Equal loading was verified by Ponceau S staining (data not shown). MagicMark (Invitrogen, Paisley, UK) protein standards were run as Mw markers. Strips were focused for 35 kVh and SDS-PAGE was performed at 200 V for approximately 1 h. Proteins were transferred to nitrocellulose membranes (Bio-Rad Laboratories). The resulting membranes were immunoblotted with antiphospho-Erk1/2 or antitotal Erk1/2 (Cell Signaling Technology, Danvers, Massachusetts, USA), followed by antirabbit horseradish peroxidase-conjugated Ab and enhanced chemiluminescence (Pierce, Rockford, Illinois, USA). Chemiluminescence images were recorded using the VersaDoc-imaging system (Bio-Rad Laboratories). Densitometric analysis of the images was performed by Quantity One Software v 4.4.0 (Bio-Rad Laboratories).

Magnetic resonance imaging

Wild type and littermate TNF^{ARE} mice were anaesthetised with isoflurane (IsoFlo, Abbott, Illinois, USA) administered in a mixture of 30% O₂ and 70% N₂. During immobilisation, isoflurane levels were kept at 3%. The dose was gradually lowered to 1.5%. Mice were submitted to a longitudinal MRI study at age of 1, 2, 3 and 5 months. MRI was performed on a 9.4 Tesla MR system (BRUKER, Ettlingen, Germany). Coronal T₁-weighted 2D images of the sacroiliac joints were acquired with a FLASH sequence: TE=3.4 ms, TR=200 ms, FA=40°, FOV=15 mm, image matrix (256×256), 16 slices, slice thickness =0.5 mm. T₂-weighted images were acquired with a RARE sequence: TE=36 ms, TR=3000 ms, ETL=8, FOV=19.2 mm, image matrix (256×192), 8 slices, slice thickness =1 mm. To compare the T₂-weighted signal intensities of the iliac bone among animals and age, relative signal intensities of the iliac bone with respect to the mean signal intensity of the muscle tissue close to the ilium bone were calculated.

Micro-CT acquisitions

Samples (n=36) were scanned in a GE Healthcare eXplore Locus SP preclinical micro-CT specimen scanner (GE Medical Systems, London, Ontario) with the following acquisition parameters: 80 kV tube voltage, 80 microamperes tube current, 1×1 detector binning, three times magnification, 500 projections acquired over 200°s using a 0.4° step size, 3000 ms exposure time and frame averaging of 4. The acquired projections were reconstructed into a 500×500×940 matrix, with 8-µm voxel size, by proprietary software (eXplore Reconstruction Utility, GE Medical Systems, London, Ontario) using a Feldkamp-type algorithm with Parker's weighting function.¹⁵ Each reconstructed micro-CT image was visually and quantitatively analysed by MicroView software (GE Medical Systems). Quantitative analysis was done by drawing a volume of interest. Bone mineral density was calculated inside this region after measuring the threshold for non-bone versus bone tissue, with the threshold value automatically determined.

A second set of micro-CT scans were performed at the Centre for X-ray Tomography of the Ghent University.¹⁶ To improve soft tissue contrast, the mice legs were immersed in a 4% HgCl₂ aqueous solution for 24 h before scanning.³¹ The mice legs were scanned using the transmission head of a dual head x-ray tube from Feinfocus (FXE 160.51), operated at 120 kV and a Varian 2520 V Paxscan flat panel detector. A beam filtration of 1 mm aluminium was applied. For each scan, 1441 projections were recorded, covering 360°, with an exposure time of 2 s per projection. The resulting voxel size was 6.5 µm. Reconstruction of the projection data was done using Octopus, a reconstruction software package developed at UGCT.¹⁷

Statistics

The non-parametric Kruskal–Wallis test or parametric ANOVA was used for comparison of three groups. The Mann–Whitney test was used for comparison of two groups. Results were considered statistically significant with two-sided p values <0.05. Regression analysis was performed to determine the correlation between osteophyte size and clinical score, irrespective of tail suspension, with R² the adjusted correlation coefficient.

RESULTS

Features of spondyloarthritis in TNF^{ARE} mice

As the precise sites where inflammation originates in SpA remain a matter of debate, a detailed clinical and histological

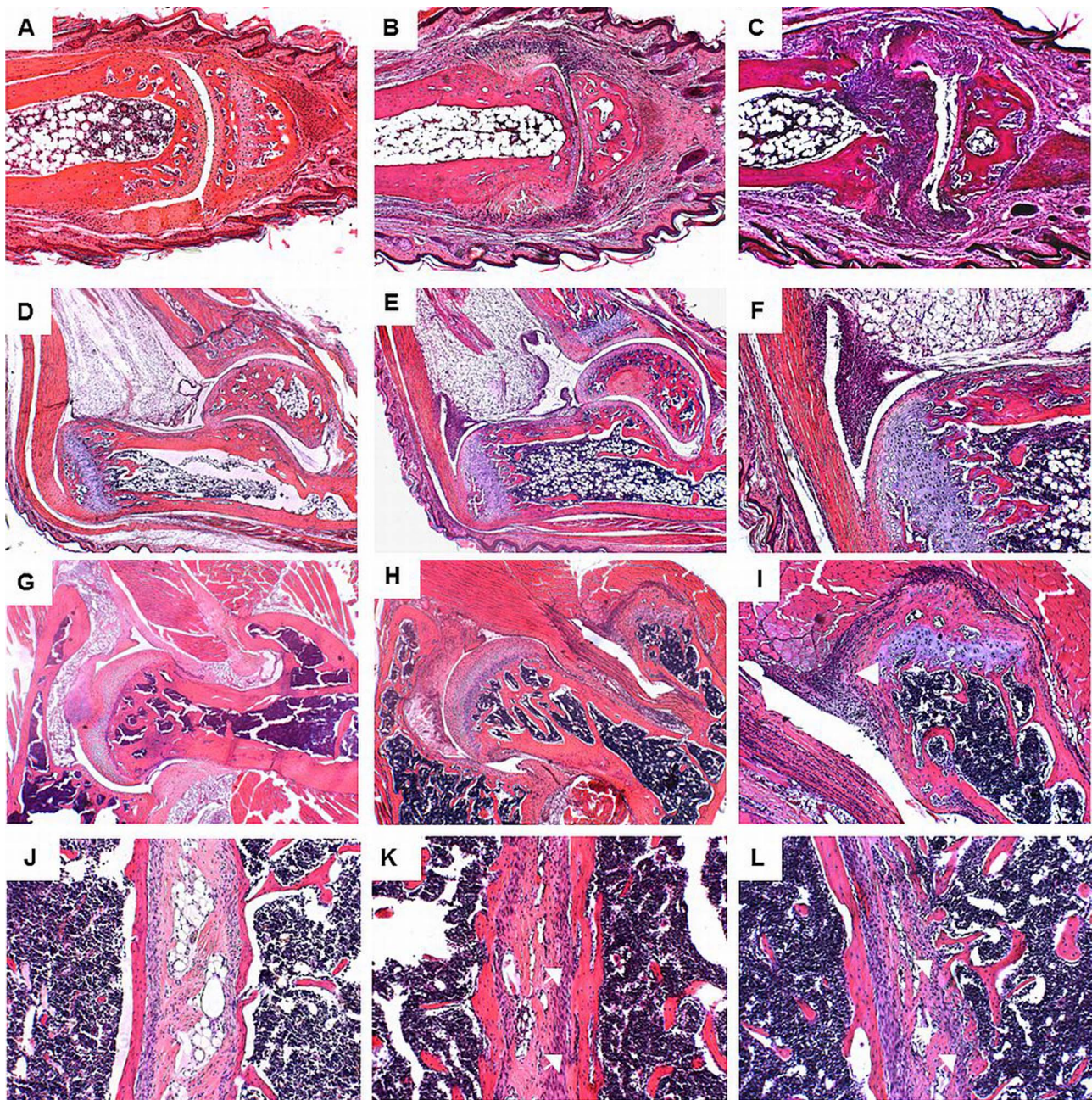
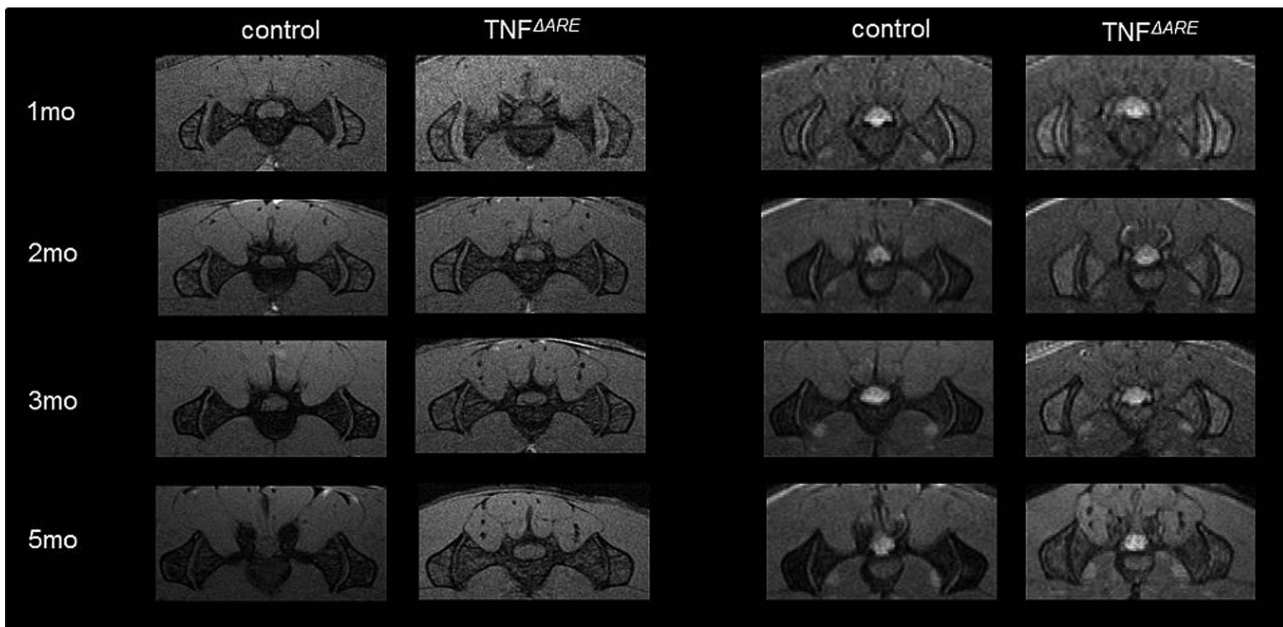


Figure 1 Features of spondyloarthritis in $TNF^{\Delta ARE}$ mice: enthesial inflammation. (A) Hind paw distal interphalangeal joint of healthy control mouse. (B) Early signs of enthesitis in hind paw of $TNF^{\Delta ARE}$ mouse. (C) Advanced erosive stage. (D) Achilles tendon of healthy control mouse. (E and F) Achilles enthesitis in $TNF^{\Delta ARE}$ mouse. (G) Hip joint of healthy control mouse. (H and I) Hip joint of $TNF^{\Delta ARE}$ mouse, arrow head points at inflammation around the greater trochanter. (J) Sacroiliac joint of a healthy control mouse. (K) Sacroiliac joint of young $TNF^{\Delta ARE}$ mouse. (L) Advanced stage sacroiliitis in $TNF^{\Delta ARE}$ mouse, white arrows point at erosions. Staining with H&E. Original magnification $\times 100$, except D, E, G and H original magnification $\times 40$. Access the article online to view this figure in colour.

study was undertaken in $TNF^{\Delta ARE}$ mice. Therefore, mice were scored every other day for arthritis development, and were sacrificed at different ages (4, 8, 12, 24 weeks) for histological assessment. In hind paws of $TNF^{\Delta ARE}$ mice, inflammation initiated at approximately 4 weeks of age within the collateral ligaments of interphalangeal joints (figure 1B), within the synovio-enthesal complex of the Achilles tendon (figure 1E,F) and the greater trochanter ligament of the hip (figure 1H,I). By the age of 6–8 weeks, inflammation spreads out into the synovium with pannus formation, and finally involves the entire joint, with bone erosions (figure 1C). Thus, articular inflammation initiates within the enthesal regions in $TNF^{\Delta ARE}$ mice.

Another interesting hallmark of the disease is the development of spinal inflammation with sacroiliitis (figure 1J–L).¹³ The joints between the sacrum and the pelvic ilium bone are joined by several ligaments and consist of a lower fibrocartilagenous part and an upper ligamentous part. As such, this region is also prone to mechanical strain. As sacroiliac joints are difficult to assess clinically, we performed a longitudinal *in vivo* MRI study, in which $TNF^{\Delta ARE}$ mice and controls were scanned monthly, starting at the age of 4 weeks, and each month both T1 and T2 sequences were run (figure 2A). On T1 sequences, progressive narrowing of joint space and irregular articular surfaces reflected progressive structural damage. On T2 sequences, the relative signal intensity

A



B

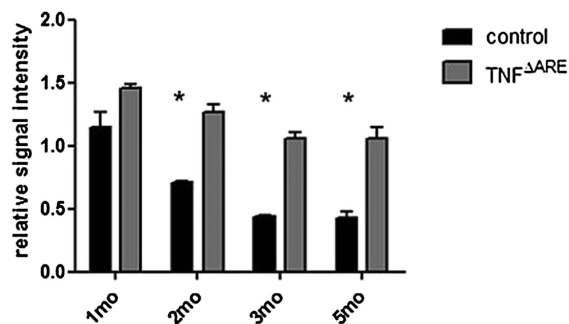


Figure 2 Consecutive monthly in vivo MRI of sacroiliac joints of healthy control and littermate TNF Δ ARE mice. (A) T1-weighted images (left panel) illustrate the development of sacroiliitis in TNF Δ ARE mice: joint space narrowing, irregular surfaces. T2-weighted images (right panel) illustrate the persistence of red marrow and general osteopenia in TNF Δ ARE mice. (B) Graph gives the relative T2-weighted signal intensities of the ilium with respect to a neighbouring muscle control region for control and TNF Δ ARE mice and for different ages. A two-way ANOVA demonstrates differences in relative signal intensities between the group of control mice and TNF Δ ARE mice, and for the different ages of the mice (*= $p < 0.05$).

of the iliac bone was calculated for each mouse (figure 2B). The signal intensity in control mice clearly decreased with age because of an increase in mineral content (63% decrease at 5 months compared with 1 month). The signal intensity in TNF Δ ARE mice only decreased by 29% between 1 and 5 months of age. This may reflect an increased water content (or bone marrow oedema) and a smaller mineral content in TNF Δ ARE mice. Alternatively, the differences in signal may also reflect the persistence of red marrow (ie, increased cellularity) seen in TNF overexpression models.¹⁸ The two-way analysis of variance (ANOVA) of relative signal intensity of the iliac bone values demonstrated both a significant main group effect (TNF Δ ARE mice vs controls) and age effect. At the age of 2, 3 and 5 months, the relative signal intensities of the TNF Δ ARE mice were significantly higher compared with the controls (figure 2B). Detailed images obtained by this in vivo imaging approach provide a valuable tool to study sacroiliitis development and allow the monitoring of therapeutic interventions in animal models for SpA. Collectively, these data highlight that inflammation occurring in TNF Δ ARE mice is highly reminiscent of human SpA.

Enthesitis occurs independent of mature T and B cells

It was recently shown that interleukin (IL)-23 responsive CD3⁺CD4⁻CD8⁻ enthesal resident T cells are essential to induce enthesitis in an IL-23 overexpression model.¹⁹ To assess the role of adaptive immunity, we backcrossed TNF Δ ARE mice on to RAG-1 deficient animals that have no mature T cells, and assessed severity of enthesitis. In RAG-1 deficient TNF Δ ARE mice, incidence of enthesitis was similar to that in T cell sufficient TNF Δ ARE mice and occurred in all mice examined (figure 3B,C). This finding highlights that both T cell dependent and independent mechanisms, most likely involving stromal cells, can contribute to enthesitis. Our data corroborate the previous role for stromal cells in TNF driven joint inflammation.¹³

Hind limb unloading inhibits development of enthesitis in TNF Δ ARE mice

We hypothesised that continuous mechanical strain caused by normal animal activity could be at the origin of enthesitis in this model. The Achilles tendon was chosen as the focus of interest for this study. To address this we used an established model for

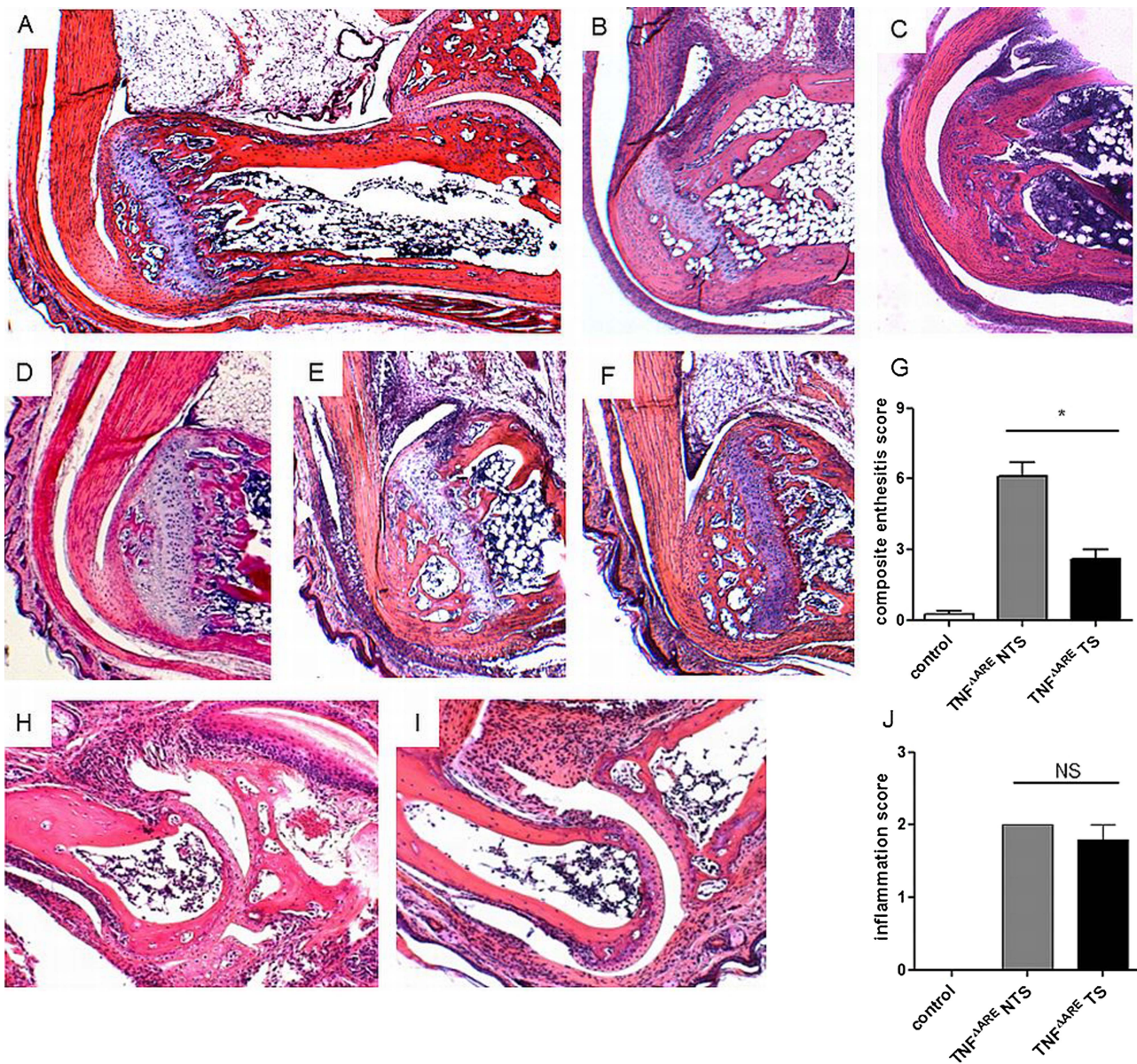


Figure 3 Inflammation at the synovio-entheseal complex is driven by biomechanical factors in TNF^{ΔARE} mice. (A) Healthy control mouse: overview of ankle. (B) Achilles tendon from a RAG-1 deficient TNF^{ΔARE} mouse. (C) Achilles tendon from RAG-1 sufficient (heterozygous) littermate TNF^{ΔARE} mouse. (D) Achilles tendon of 4-week-old healthy control mouse. (E) Non-tail suspended TNF^{ΔARE} mouse. (F) Littermate TNF^{ΔARE} mouse subjected to tail suspension for 14 days continuously. (G) Composite histology score demonstrates reduced severity of enthesitis upon tail suspension, **p*<0.05. (H) Distal interphalangeal joint in front paw of a non-tail suspended TNF^{ΔARE} and (I) tail suspended TNF^{ΔARE} mouse. All original magnification ×40. (J) Graph demonstrates inflammation score in front paws from a subgroup of mice from tail suspension experiments, N=4 in each group, values are mean and SEM. Access the article online to view this figure in colour.

hind limb unloading, tail suspension.^{20 21} In specially designed cages, TNF^{ΔARE} mice and healthy controls were tail suspended, and clinical signs of arthritis were assessed daily. Hind limb unloading was initiated before the known onset of illness, before 4 weeks of age, in a preventive setting. Following a 14-day period of unloading, none of the mice subjected to this procedure displayed clinical signs of peripheral arthritis of ankles and hind paws, whereas all control mice that were not tail suspended, did. Furthermore, by detailed histological analysis, we detected only minor inflammatory changes in tail suspended TNF^{ΔARE} mice, but significantly more inflammation in their weight bearing controls (figure 3D–G). In a subgroup of mice, arthritis was also evaluated in front paws. In general, severity of inflammation did not differ between weight carrying

front paws of tail-suspended and control mice (figure 3H–J). These data strongly suggest that the onset of enthesitis in this animal model is driven by mechanical load on hind paws.

Mechanical stress triggers Erk1/2 signalling in TNF^{ΔARE} mice

Activation of mitogen-activated protein kinase (MAPK) signalling pathways was previously demonstrated as a response to stretch in a variety of stromal cell types.^{22–25} Therefore, we performed a tail suspension study, whereby TNF^{ΔARE} mice were subjected to tail suspension for 7 days, again in a preventive setting, before the onset of enthesitis. Tail suspended mice did not show signs of clinical arthritis, as compared with weight bearing controls. Seven days later, half of the group of mice were allowed to walk around for 10 min before they were sacrificed. Induction of

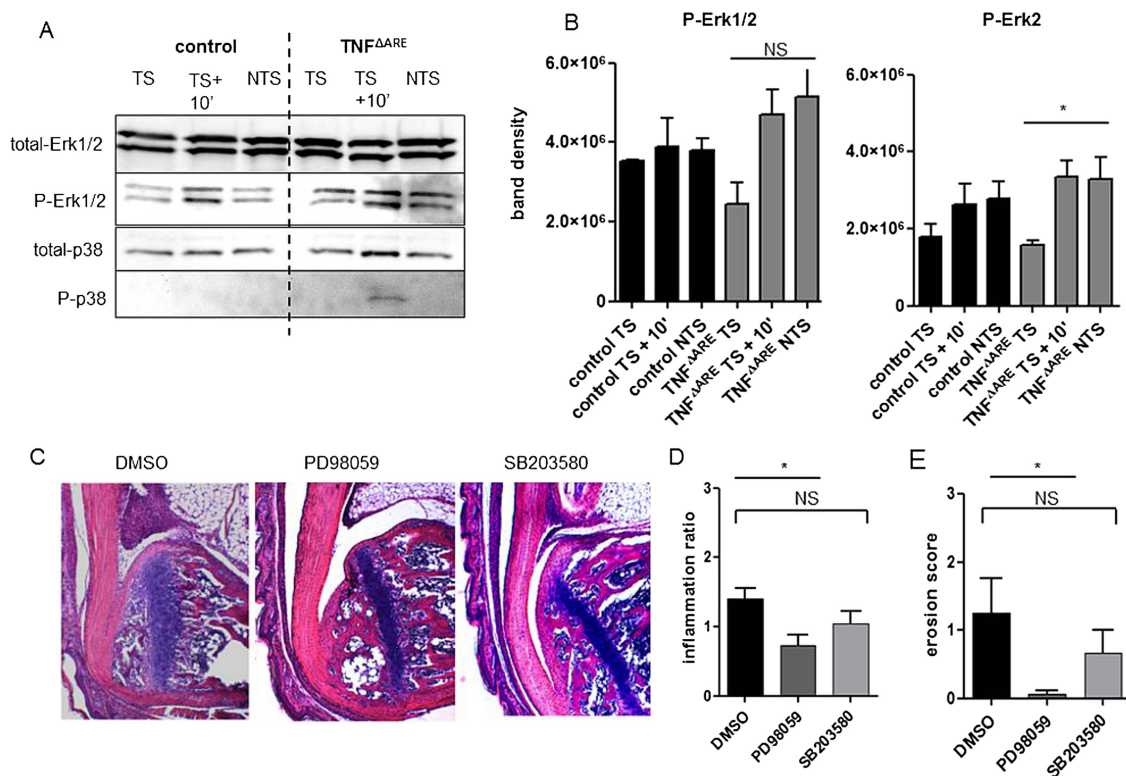


Figure 4 Erk1/2 signalling is involved in enthesitis development in TNF^{ΔARE} mice. (A) Western blotting on Achilles tendon lysates of 4-week-old tail suspended (7 days) and non-tail suspended healthy control and TNF^{ΔARE} mice. Half of the group of tail suspended mice was allowed to walk around for 10 min before they were sacrificed. Figure shows one representative experiment out of three. (B) Densitometric analysis of the images was performed by Quantity One Software. N=5 mice per condition, **p*<0.05. (C) H&E staining of the Achilles tendon and ankle of 4-week-old TNF^{ΔARE} mice treated with PD98059, SB203580 or DMSO for 7 days. (D) Inflammation within the synovio-entheseal complex (SEC) was scored by digital image analysis, and is shown as the ratio of the inflamed area within the SEC and the area of the growth plate. (E) The extent of erosion of the calcaneal bone was scored by two blinded assessors. N=3–5 mice in each group. Values are means and SEM. **p*<0.05. Access the article online to view this figure in colour.

phosphorylated-Erk1/2 (P-Erk1/2), phosphorylated-Jnk (P-Jnk) and phosphorylated-p38 (P-p38) was assessed by western blotting on Achilles tendon lysates. As figure 4A indicates, in Achilles tendon lysates from wild type mice subjected to tail suspension, P-Erk1/2 was comparable with weight bearing wild type mice, while the reintroduction of mechanical strain during 10 min resulted in a small albeit not significant induction of P-Erk1/2. By contrast, in TNF^{ΔARE} Achilles tendon, a manifest increase of P-Erk1/2 could be detected upon 10 min of weight bearing, with significant induction of P-Erk2 on densitometry (figure 4B). No significant signal of P-p38 was detected, and P-Jnk was not detected at all (not shown).

MAPK inhibition interferes with tendinitis development

Small molecular inhibitors of MAPK pathways whose activity has previously been assessed *in vitro* and *in vivo* were selected. The selective Erk1/2/MEK1 inhibitor PD98059 was used to inhibit Erk1/2 signalling, and SB203580 was used for p38 pathway inhibition^{26 27} (and own unpublished data); 4-week-old TNF^{ΔARE} mice were injected intraperitoneally with inhibitors (50 μg/g) or vehicle (dimethylsulphoxide (DMSO)) for seven consecutive days, and development of arthritis was assessed daily. Detailed histological analysis of H&E stained ankles using digital image analysis showed marked reduction in inflammation within the synovio-entheseal complex in mice treated with PD98059 (figure 4C,D). In addition, there was significantly less calcaneal bone erosion in mice treated with PD98059 versus control mice (figure 4E). These findings indicate that blockade of the Erk1/2 signalling pathway altered the development of enthesitis.

Inflammation within the ileum, another disease manifestation in TNF^{ΔARE} mice, was not altered significantly upon treatment with MAPK inhibitors (data not shown).

New bone formation

New bone formation, an important feature of human spondyloarthritis, does not appear in TNF^{ΔARE} mice, consistent with previous work by Diarra *et al*²⁸ performed in the human TNF transgenic (hTNFtg) mouse model. TNF was shown to be the major inducer of Dickkopf-1 (DKK-1), a regulatory molecule of the Wnt pathway, which operated as a brake on new bone formation. In addition, blockade of DKK-1 resulted in osteophyte formation within arthritic joints of hTNFtg mice. Therefore, we focused on the collagen-antibody-induced arthritis model (CAIA) to study new bone formation in relation to mechanical stress. CAIA was induced in susceptible DBA/1 mice as described.^{29 30} As early as 7 days after immunisation, CAIA mice exhibit enthesitis which eventually evolves into a destructive polyarthritis¹⁹ (data not shown). Osteophyte formation occurs after resolution of the inflammatory phase. When a full blown clinical arthritis was established at day 10 after immunisation, half of the group of mice were tail suspended for 28 days to prevent mechanical loading on hind paws, and half were kept in normal cages. In tail suspended mice, osteophytes were significantly smaller compared with control mice, as shown by histology and micro-CT imaging (figure 5A,B). In general, osteophyte size correlated with the severity of inflammation. Mice with only minimal clinical arthritis developed no osteophytes when tail suspended, whereas mice with higher arthritis

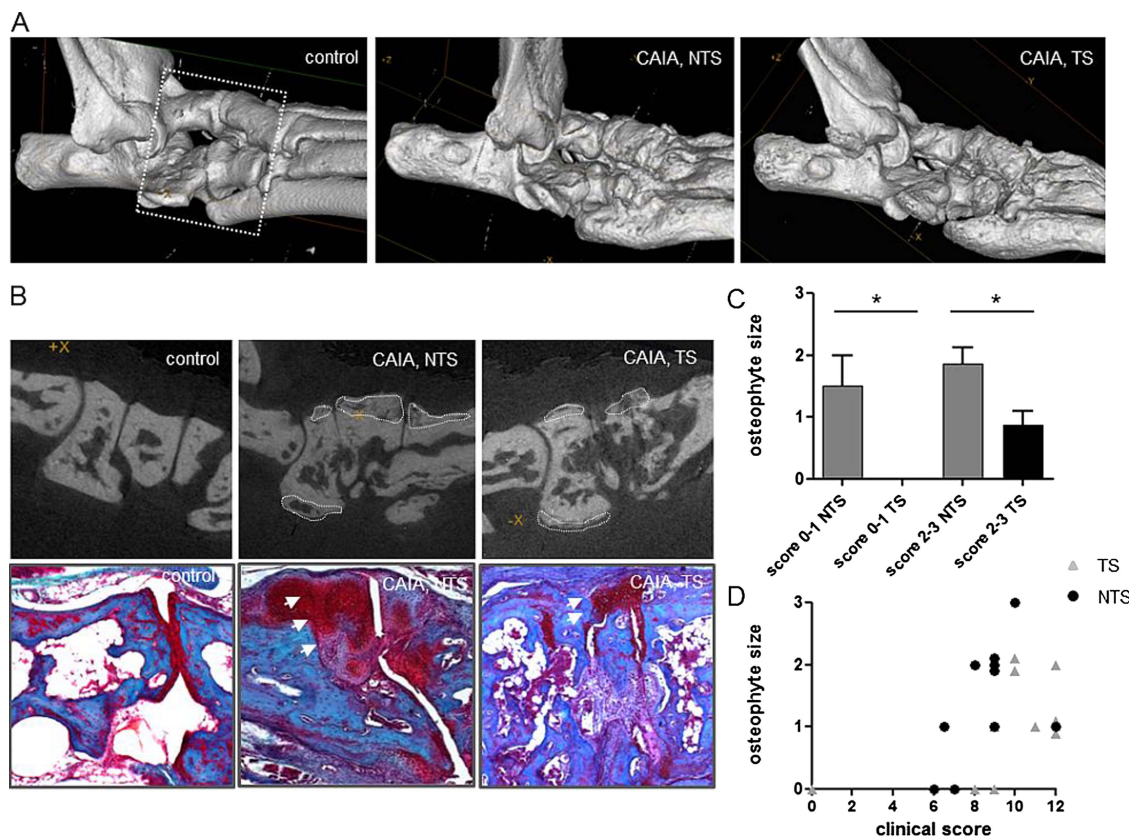


Figure 5 New bone formation is driven by mechanical strain. (A and B) Micro-CT images and corresponding H&E staining of the region within the square from healthy control, non-tail suspended and tail suspended collagen-antibody-induced arthritis mice. (C) Osteophyte size was scored by two blinded assessors. Graph shows osteophyte size for mice with minor (0–1) or major (2–3) clinical arthritis score (one paw). N=10 mice in each group, $*=p<0.05$. (D) Correlation of osteophyte size with clinical score. $R^2=0.28$, $p=0.03$. Access the article online to view this figure in colour.

scores developed significantly smaller osteophytes when tail suspended compared with non-tail suspended mice (figure 5C,D).

New bone formation occurred at distance from the joint articular surfaces. Moreover, immersion of the entire paw in mercury chloride (HgCl_2), which allows uptake in soft tissues such as tendons,³¹ followed by high resolution CT, revealed that these osteophytes are formed mainly at enthesal sites (see online supplementary figure S1 and S2). Collectively, these findings underscore a role for mechanical strain in new bone formation at enthesal sites.

DISCUSSION

It has been a great matter of debate where disease originates in SpA patients since, during the course of disease, synovium, enthesis as well as bone marrow can become involved. Due to their location at the interface of ligaments and bone, entheses are especially prone to mechanical forces. It is generally accepted although not formally proven that both mechanical and inflammatory factors can trigger enthesitis, with the enthesitis-based origin of SpA as a formal hypothesis.⁶ According to an occupational study by Ward *et al*,³² physical activities that required repetitive strain such as stretching, bending or twisting, as well as exposure to whole body vibration, were associated with more radiographic damage in ankylosing spondylitis. Yet, experimental evidence supporting these theories was lacking. We provide evidence for a mechanotransduction-associated origin of enthesitis and new bone formation at enthesal sites.

First, enthesitis is an early disease feature in TNF^{AARE} mice. Hind limb unloading prevented the onset of Achilles enthesitis

in TNF^{AARE} mice. Front paws of tail suspended TNF^{AARE} mice showed similar arthritis severity compared with weight bearing controls, although the body weight of these mice was loaded on the front paws. However, careful observation revealed that tail suspended mice tended to move less than the control group, which provides an explanation for the contra-intuitive finding that severity of inflammation in front paws does not increase after tail suspension and hind limb unloading. We hypothesise that minimal biomechanical stress is sufficient to induce a sustained inflammatory response. Thus, biomechanical stress rather functions as an on/off switch and there is not necessarily a linear relationship between the amount of stress and the degree of inflammation, at least not above a given level of biomechanical stress. The resulting minor increase, if any, may not be detected by the scoring system, which has limited power.

Therefore, mechanical strain may be considered the trigger of an inflammatory process, and provides an explanation for the unsolved paradigm of enthesitis development in SpA.

It was previously demonstrated that in the presence of chronic TNF overexposure, signalling through TNFRI in synovial fibroblasts and intestinal myofibroblasts appears to be sufficient to develop arthritis and Crohn's-like ileitis in TNF^{AARE} mice.¹³ Therefore, crosstalk between the myeloid cell compartment and stromal cells such as fibroblasts is critically involved in the development of both the articular and the intestinal phenotype. Importantly, mature T cells are not involved in enthesitis development in TNF^{AARE} mice, as demonstrated in *RAG-1* deficient mice. This highlights that several pathways exist to induce enthesitis, some of which rely on IL-23R^+ innate-like enthesal

resident cells,¹⁹ while others are strictly dependent upon stromal cell function. In more complex situations such as in SpA patients, both T cell dependent and independent mechanisms may exist and could have additive effects.

Mechanical stress is sensed by cells via mechanoreceptors such as integrins, and transmitted through MAPK signalling pathways.³³ In this study, activation of Erk1/2 signalling pathways in Achilles tendon lysates could be efficiently prohibited by hind limb unloading, while reintroduction of mechanical strain resulted in immediate phosphorylation of Erk1/2 (within 10 min), both in wild type and TNF^{ARE} tendons. Small molecular MAPK inhibitors were proven effective in animal models for arthritis, and may be promising therapeutic targets in treatment of inflammatory diseases.^{34–35} However, limited data are available on treatment options of enthesitis in particular. In the present study, the effects of an Erk1/2 inhibitor and a p38 inhibitor on enthesitis development were evaluated. With Erk1/2 inhibition, we detected a clear decrease in inflammation within the synovio-entheseal complex; in addition, there was a significant reduction in calcaneal bone erosion.

The MAPK pathways have previously been shown to modulate TNF biosynthesis, and TNF signalling is involved both upstream and downstream of MAPK activation.³⁶ In particular, the adenosine uracil (AU) rich elements within the TNF transcript are known targets for p38-mediated activation of TNF translation upon lipopolysaccharide stimulation.¹² In addition, the Erk1/2 pathway requires the presence of ARE for post-transcriptional regulation, that is, nuclear export of the TNF message.³⁷ In wild type mice, MAPK blockade in general results in a dose dependent inhibition of TNF translation. As these targets are deleted in TNF^{ARE} mice, MAPK blockade would be unable to inhibit TNF translation via this pathway. Therefore, the observed biological effects of Erk1/2 blockade in TNF^{ARE} mice may even be underestimated and partly TNF independent. However, data from other models suggest that inhibition of MAPK has complex effects. In the ankylosing enthesitis model in DBA/1 mice, inhibition of p38 accelerated ankylosis rather than inhibiting arthritis, although in vitro data suggested an inhibitory effect of the compound used on transforming growth factor and bone morphogenetic protein induced chondro- and osteogenesis.³⁸

A second hallmark of spondyloarthritis is the occurrence of new bone formation leading to ankylosis. However, in TNF^{ARE} mice, new bone formation could never be demonstrated, presumably due to continuous and deregulated TNF production that functions as a brake on this process through for example DKK1, which is a potent inhibitor of Wnt signalling. In addition, new bone formation is much less pronounced in the CB57BL/6 background than on other backgrounds such as DBA/1. Successful inhibition of inflammation in mouse models and in patients, for instance with TNF blocking agents, does not affect ankylosis or radiographic progression.^{9–11} However, recent data suggest that long term treatment may be effective on structural changes.^{39–40} The sequence of inflammation followed by new bone formation is not formally proven, although there may be a preference for syndesmophytes to develop at inflamed vertebral edges in human SpA.^{41–42} In addition, recent MRI studies suggested that new bone formation more likely develops in advanced inflammatory spinal lesions. In these lesions, resolution of inflammation results in fat metaplasia and ultimately in new bone formation.^{43–44} Here, we demonstrated that in CAIA mice, osteophytes are significantly smaller when weight bearing is prohibited, supporting a role for mechanical strain in their development. In addition, tail suspension was able to prevent the development of osteophytes when only minimal signs of

inflammation were evident, and could minimise osteophyte size in more advanced arthritis. In general, osteophyte size correlated with the severity of inflammation. Although this particular aspect was not the focus of this study, it indirectly supports the relationship between inflammation and new bone formation.

In summary, these findings comprise the first formal proof of a new paradigm that mechanical forces are the underlying cause of enthesitis and new bone formation in SpA. This opens avenues for a new field of mechanotransduction-associated pathways in SpA.

Author affiliations

- ¹Laboratory for Molecular Immunology and Inflammation, Department of Rheumatology, University Hospital, Ghent, Belgium
- ²UGCT, Department of Physics and Astronomy, University of Ghent, Ghent, Belgium
- ³Alexander Fleming Biomedical Sciences Research Center, Vari, Greece
- ⁴Bio-Imaging Lab, University of Antwerp, Antwerp, Belgium
- ⁵Department of Radiology, University Hospital, Ghent, Belgium
- ⁶Laboratory of Tissue Homeostasis and Disease, Skeletal Biology and Engineering Center, Department of Development and Regeneration, KU Leuven, Belgium

Acknowledgements The authors wish to thank C Van Hove at INFINITY for performing and analysing micro-CT images and L Van Praet for statistical analysis.

Contributors All authors contributed to the conception and design of the study, acquisition, analysis or interpretation of data, and drafting or revising the article critically for intellectual content. All authors approved the final version for publication.

Funding This work is supported by the Fund for Scientific Research—Flanders, by a concerted action grant from Ghent University, and by the Special Research Fund of the Ghent University (BOF, GOA 01G01008). DE is part of a multidisciplinary research platform (MRP) of Ghent University and is supported by an Interuniversity Attraction Pole (Project P7/O7).

Competing interests None.

Provenance and peer review Not commissioned; externally peer reviewed.

Data sharing statement Data not shown are available upon email request to the corresponding author.

REFERENCES

- 1 Braun J, Bollow M, Remlinger G, *et al.* Prevalence of spondylarthropathies in HLA-B27 positive and negative blood donors. *Arthritis Rheum* 1998;41:58–67.
- 2 Sieper J, Rudwaleit M, Khan MA, *et al.* Concepts and epidemiology of spondyloarthritis. *Best Pract Res Clin Rheumatol* 2006;20:401–17.
- 3 McGonagle D, Gibbon W, Emery P. Classification of inflammatory arthritis by enthesitis. *Lancet* 1998;352:1137–40.
- 4 Benjamin M, McGonagle D. The anatomical basis for disease localisation in seronegative spondyloarthropathy at entheses and related sites. *J Anat* 2001;199 (Pt 5):503–26.
- 5 Machado P, Landewe R, Braun J, *et al.* Both structural damage and inflammation of the spine contribute to impairment of spinal mobility in patients with ankylosing spondylitis. *Ann Rheum Dis* 2010;69:1465–70.
- 6 McGonagle D, Stockwin L, Isaacs J, *et al.* An enthesitis based model for the pathogenesis of spondyloarthropathy additive effects of microbial adjuvant and biomechanical factors at disease sites. *J Rheumatol* 2001;28:2155–9.
- 7 McGonagle D, Lories RJ, Tan AL, *et al.* The concept of a "synovio-entheseal complex" and its implications for understanding joint inflammation and damage in psoriatic arthritis and beyond. *Arthritis Rheum* 2007;56:2482–91.
- 8 McGonagle D, Wakefield RJ, Tan AL, *et al.* Distinct topography of erosion and new bone formation in achilles tendon enthesitis: implications for understanding the link between inflammation and bone formation in spondylarthritis. *Arthritis Rheum* 2008;58:2694–9.
- 9 van der Heijde D, Salonen D, Weissman BN, *et al.* Assessment of radiographic progression in the spines of patients with ankylosing spondylitis treated with adalimumab for up to 2 years. *Arthritis Res Ther* 2009;11:R127.
- 10 van der Heijde D, Landewe R, Baraliakos X, *et al.* Radiographic findings following two years of infliximab therapy in patients with ankylosing spondylitis. *Arthritis Rheum* 2008;58:3063–70.
- 11 van der Heijde D, Landewe R, Einstein S, *et al.* Radiographic progression of ankylosing spondylitis after up to two years of treatment with etanercept. *Arthritis Rheum* 2008;58:1324–31.
- 12 Kontoyiannis D, Pasparakis M, Pizarro TT, *et al.* Impaired on/off regulation of TNF biosynthesis in mice lacking TNF AU-rich elements: implications for joint and gut-associated immunopathologies. *Immunity* 1999;10:387–98.

- 13 Armaka M, Apostolaki M, Jacques P, *et al.* Mesenchymal cell targeting by TNF as a common pathogenic principle in chronic inflammatory joint and intestinal diseases. *J Exp Med* 2008;205:331–7.
- 14 Jacques P, Venken K, Van Beneden K, *et al.* Invariant natural killer T cells are natural regulators of murine spondylarthritis. *Arthritis Rheum* 2010;62:988–99.
- 15 Parker DL. Optimal short scan convolution reconstruction for Fanbeam Ct. *Med Phys* 1982;9:254–7.
- 16 Masschaele BC, Cnudde V, Dierick M, *et al.* UGCT: new x-ray radiography and tomography facility. *Nucl Instrum Meth A* 2007;580:266–9.
- 17 Vlassenbroeck J, Dierick M, Masschaele B, *et al.* Software tools for quantification of X-ray microtomography. *Nucl Instrum Meth A* 2007;580:442–5.
- 18 Proulx ST, Kwok E, You Z, *et al.* Elucidating bone marrow edema and myelopoiesis in murine arthritis using contrast-enhanced magnetic resonance imaging. *Arthritis Rheum* 2008;58:2019–29.
- 19 Sherlock JP, Joyce-Shaikh B, Turner SP, *et al.* IL-23 induces spondyloarthritis by acting on ROR-gamma+ CD3+CD4-CD8- enthesal resident T cells. *Nat Med* 2012;18:1069–76.
- 20 Morey-Holton ER, Globus RK. Hindlimb unloading of growing rats: a model for predicting skeletal changes during space flight. *Bone* 1998;22(Suppl):83S–8S.
- 21 Morey-Holton ER, Globus RK. Hindlimb unloading rodent model: technical aspects. *J Appl Physiol* 2002;92:1367–77.
- 22 Cornelissen J, Armstrong J, Holt CM. Mechanical stretch induces phosphorylation of p38-MAPK and apoptosis in human saphenous vein. *Arterioscler Thromb Vasc Biol* 2004;24:451–6.
- 23 Correa-Meyer E, Pesce L, Guerrero C, *et al.* Cyclic stretch activates ERK1/2 via G proteins and EGFR in alveolar epithelial cells. *Am J Physiol Lung Cell Mol Physiol* 2002;282:L883–91.
- 24 Lal H, Verma SK, Smith M, *et al.* Stretch-induced MAP kinase activation in cardiac myocytes: differential regulation through beta1-integrin and focal adhesion kinase. *J Mol Cell Cardiol* 2007;43:137–47.
- 25 Papakrivopoulou J, Lindahl GE, Bishop JE, *et al.* Differential roles of extracellular signal-regulated kinase 1/2 and p38MAPK in mechanical load-induced procollagen alpha1(I) gene expression in cardiac fibroblasts. *Cardiovasc Res* 2004;61:736–44.
- 26 Alessi DR, Cuenda A, Cohen P, *et al.* PD 098059 is a specific inhibitor of the activation of mitogen-activated protein kinase kinase in vitro and in vivo. *J Biol Chem* 1995;270:27489–94.
- 27 Cuenda A, Rouse J, Doza YN, *et al.* SB 203580 is a specific inhibitor of a MAP kinase homologue which is stimulated by cellular stresses and interleukin-1. *FEBS letters* 1995;364:229–33.
- 28 Diarra D, Stolina M, Polzer K, *et al.* Dickkopf-1 is a master regulator of joint remodeling. *Nat Med* 2007;13:156–63.
- 29 Nandakumar KS, Holmdahl R. Efficient promotion of collagen antibody induced arthritis (CAIA) using four monoclonal antibodies specific for the major epitopes recognized in both collagen induced arthritis and rheumatoid arthritis. *J Immunol Methods* 2005;304:126–36.
- 30 Nandakumar KS, Andren M, Martinsson P, *et al.* Induction of arthritis by single monoclonal IgG anti-collagen type II antibodies and enhancement of arthritis in mice lacking inhibitory Fc gammaRIIB. *Eur J Immunol* 2003;33:2269–77.
- 31 Pauwels E, Van Loo D, Cornillie P, *et al.* An exploratory study of contrast agents for soft tissue visualization by means of high resolution X-ray computed tomography imaging. *J Microsc* 2013;250:21–31.
- 32 Ward MM, Reveille JD, Learch TJ, *et al.* Occupational physical activities and long-term functional and radiographic outcomes in patients with ankylosing spondylitis. *Arthritis Rheum* 2008;59:822–32.
- 33 Knies Y, Bernd A, Kaufmann R, *et al.* Mechanical stretch induces clustering of beta1-integrins and facilitates adhesion. *Exp Dermatol* 2006;15:347–55.
- 34 Thiel MJ, Schaefer CJ, Lesch ME, *et al.* Central role of the MEK/ERK MAP kinase pathway in a mouse model of rheumatoid arthritis: potential proinflammatory mechanisms. *Arthritis Rheum* 2007;56:3347–57.
- 35 Mihara K, Almansa C, Smeets RL, *et al.* A potent and selective p38 inhibitor protects against bone damage in murine collagen-induced arthritis: a comparison with neutralization of mouse TNFalpha. *Br J Pharmacol* 2008;154:153–64.
- 36 Schett G, Tohidast-Akrad M, Smolen JS, *et al.* Activation, differential localization, and regulation of the stress-activated protein kinases, extracellular signal-regulated kinase, c-JUN N-terminal kinase, and p38 mitogen-activated protein kinase, in synovial tissue and cells in rheumatoid arthritis. *Arthritis Rheum* 2000;43:2501–12.
- 37 Skinner SJ, Deleault KM, Fecteau R, *et al.* Extracellular signal-regulated kinase regulation of tumor necrosis factor-alpha mRNA nucleocytoplasmic transport requires TAP-NxT1 binding and the AU-rich element. *J Biol Chem* 2008;283:3191–9.
- 38 Braem K, Luyten FP, Lories RJ. Blocking p38 signalling inhibits chondrogenesis in vitro but not ankylosis in a model of ankylosing spondylitis in vivo. *Ann Rheum Dis* 2012;71:722–8.
- 39 Baraliakos X, Haibel H, Listing J, *et al.* Continuous long-term anti-TNF therapy does not lead to an increase in the rate of new bone formation over 8 years in patients with ankylosing spondylitis. *Ann Rheum Dis* Published Online First: 27 Mar 2013. doi:10.1136/annrheumdis-2012-202698.
- 40 Haroon N, Inman RD, Learch TJ, *et al.* The impact of TNF-inhibitors on radiographic progression in ankylosing spondylitis. *Arthritis Rheum* Published Online First: 1 Jul 2013. doi:10.1002/art.38070. *ACR abstract 782*. 2012.
- 41 van der Heijde D, Machado P, Braun J, *et al.* MRI inflammation at the vertebral unit only marginally predicts new syndesmophyte formation: a multilevel analysis in patients with ankylosing spondylitis. *Ann Rheum Dis* 2012;71:369–73.
- 42 Maksymowych WP, Chiowchanwisawakit P, Clare T, *et al.* Inflammatory lesions of the spine on magnetic resonance imaging predict the development of new syndesmophytes in ankylosing spondylitis: evidence of a relationship between inflammation and new bone formation. *Arthritis Rheum* 2009;60:93–102.
- 43 Maksymowych WP, Morency N, Conner-Spady B, *et al.* Suppression of inflammation and effects on new bone formation in ankylosing spondylitis: evidence for a window of opportunity in disease modification. *Ann Rheum Dis* 2013;72:23–8.
- 44 Chiowchanwisawakit P, Lambert RG, Conner-Spady B, *et al.* Focal fat lesions at vertebral corners on magnetic resonance imaging predict the development of new syndesmophytes in ankylosing spondylitis. *Arthritis Rheum* 2011;63:2215–25.